www.czasopisma.pan.pl PAN POLSKA AKADEMIA NAUK www.journals.pan.pl

Arch. Metall. Mater. **63** (2018), 3, 1555-1564

DOI: 10.24425/123847

W. WOŁCZYŃSKI*#

PATTERN SELECTION IN THE FRAME OF THERMODYNAMIC SIMILARITY BETWEEN EUTECTICS: Cu-Cu_2O AND (Zn)-$Zn_{16}Ti$ – EXPERIMENT

Coagulation and solidification of the copper droplets suspend in the liquid slag are usually accompanied by the appearance of the Cu-Cu_2O eutectic. Locally, this eutectic is created in the stationary state. Therefore, frequently it has a directional morphology. Since the E = (Zn) + $Zn_{16}Ti$ – eutectic is similar in the asymmetry of the phase diagram to the Cu-Cu_2O – eutectic, the (Zn) single crystal strengthened by the E = (Zn) + $Zn_{16}Ti$ precipitate is subjected to directional growth by the *Bridgman's* system and current analysis. Experimentally, the strengthening layers (stripes) are generated periodically in the (Zn) – single crystal as a result of the cyclical course of precipitation which accompanies the directional solidification. These layers evince diversified eutectic morphologies like irregular rods, regular lamellae, and regular rods. The L – shape rods of the $Zn_{16}Ti$ – intermetallic compound appear within the first range of the growth rates when the irregular eutectic structure is formed. Next, the branched rods transform into regular rods and subsequently the regular rods into regular lamellae transitions can be recorded. The regular lamellae exist only within a certain range of growth rates. Finally, the regular rods re-appear at some elevated growth rates.

The entropy production per unit time and unit volume is calculated for the regular eutectic growth. It will allow to formulate the entropy production per unit time for both eutectic structure: rod-like and lamellar one.

Keywords: Minimum entropy production; Regular eutectics; Irregular eutectics, Droplets coagulation; Thermodynamic competition

1. Introduction

The phenomenon of strengthening is incessantly observed in the (Zn) – single crystal with small addition of titanium, [1]. The strengthening results from the presence of the regular layers situated horizontally in a single crystal growing up. Every layer consists of two eutectic phases: first is the (Zn) – phase, the same as the matrix of the single crystal, second is the $Zn_{16}Ti$ – intermetallic compound.

The (Zn) – single crystal is usually produced in the *Bridgman's* system with the imposed both the positive thermal gradient and constant growth rate. The range of growth rates within which the single crystal formation is possible can be successfully extended. However, an addition of a small quantity of copper to the Zn-Ti alloy used in the experiment is required, [2]. The added copper modifies the specific surface free energy at the solid/liquid (s/l) interface, especially at its triple point. On the other hand, copper does not form any intermetallic compound with zinc. Copper is usually dissolved in the zinc-titanium solid solution.

Additionally, the Ti – solute redistribution emerges in the (Zn) – single crystal matrix situated between neighboring layers. The intensity of the solute redistribution depends directly on the growth rate and especially on the activity / intensity of the back-diffusion. The Ti – solute redistribution created in the single crystal matrix (between neighboring layers) also influences the (Zn) – single crystal properties.

It is postulated that the thermodynamics of irreversible processes is able to explain / justify the structural transformations. Thus, a new criterion is formulated to describe eutectic morphologies competition which results in the appearance of the wining structure. The criterion is: ***in the structural – thermodynamic competition the winner is this kind of the pattern for which minimum entropy production is lower***, [3,4].

2. Strengthening layer morphology

Strengthening of an alloy through other phases is well known and was a subject of the theoretical explanation, [5]. Some experimental observations confirm the fact that an alloy gets hardening by the appearance of some phases precipitated during heat treatment or solidification, [6-10].

The current experiments also lead to the improvement of mechanical properties, as mentioned. The experiments were performed in the *Bridgman's* system with the moving temperature

* INSTITUTE OF METALLURGY AND MATERIALS SCIENCE, POLISH ACADEMY OF SCIENCES, 30-059 KRAKÓW, UL. REYMONTA 25, POLAND

Corresponding author: w.wolczynski@imim.pl

field. The system was equipped with the graphite crucible of the sophisticated geometry. It allowed to locate a (Zn) – crystal seed of the desired crystallographic orientation. Moreover, the argon protective atmosphere was applied to the *Bridgman's* system. The following alloys were subjected to the oriented growth: Zn-0.01Ti, (Fig. 1); Zn-0.02Ti (Fig. 2); Zn-0.1Ti (Fig. 3); and additionally Zn-0.1Ti-0.1Cu; Zn-0.2Ti-0.15Cu [wt.%] to extend the range of applicable growth rates. As a matter of fact, all these alloys are located near the eutectic point of the Zn-$Zn_{16}Ti$ – phase diagram even if a very small addition of titanium is inserted, Fig. 4a. In the case of the metallurgical practice connected with the Cu-O system, Fig. 4b, often the refining is applied to the Cu-0,6O or even to the Cu-0,9O material.

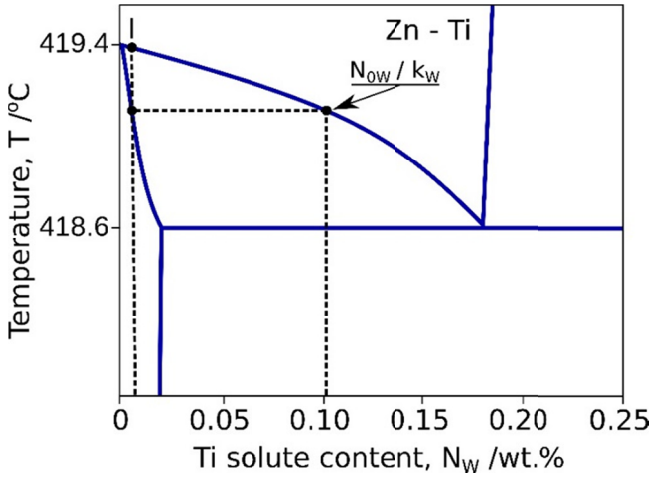

Fig. 1. The nominal Ti – solute concentration ("I"), $N_{0W} \equiv I = 0.01$, [wt.%], and the position of the $I \rightarrow N_{0W}/k_W$ – path for the equilibrium solidification

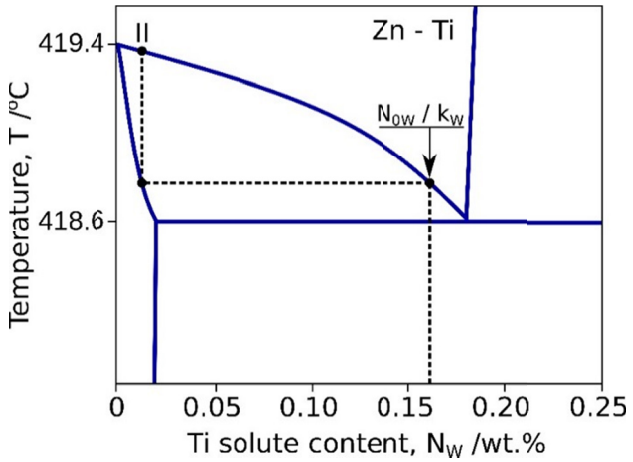

Fig. 2. The nominal Ti – solute concentration ("II"), $N_{0W} \equiv II = 0.02$, [wt.%], and the position of the $II \rightarrow N_{0W}/k_W$ – path for the equilibrium solidification

Titanium solubility in the (Zn) – solid solution is about 0.000546 [at.%] at the ambient temperature, but it reaches 0.0204 [at.%] at 300 [°C], and 0.027 [at.%] at 400 [°C]. The eutectic point is located at 418.6 [°C] with titanium concentration equal to 0.25 [at.%] (0.18 [wt.%], Fig. 4a).

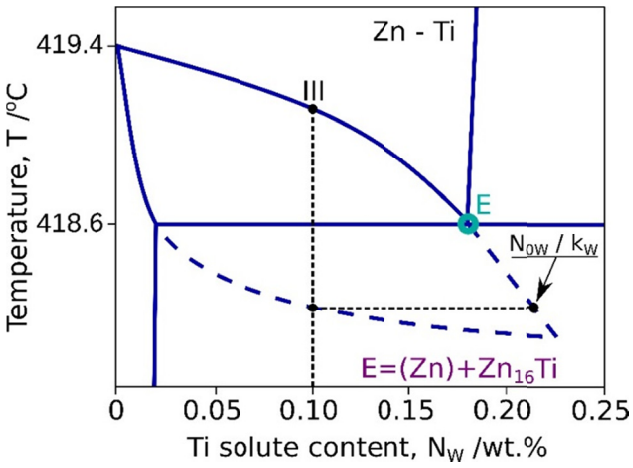

Fig. 3. The nominal Ti – solute concentration ("III"), $N_{0W} \equiv III = 0.1$, [wt.%], and the position of the $III \rightarrow E \rightarrow N_{0W}/k_W$ – path for the equilibrium solidification (partially speculative)

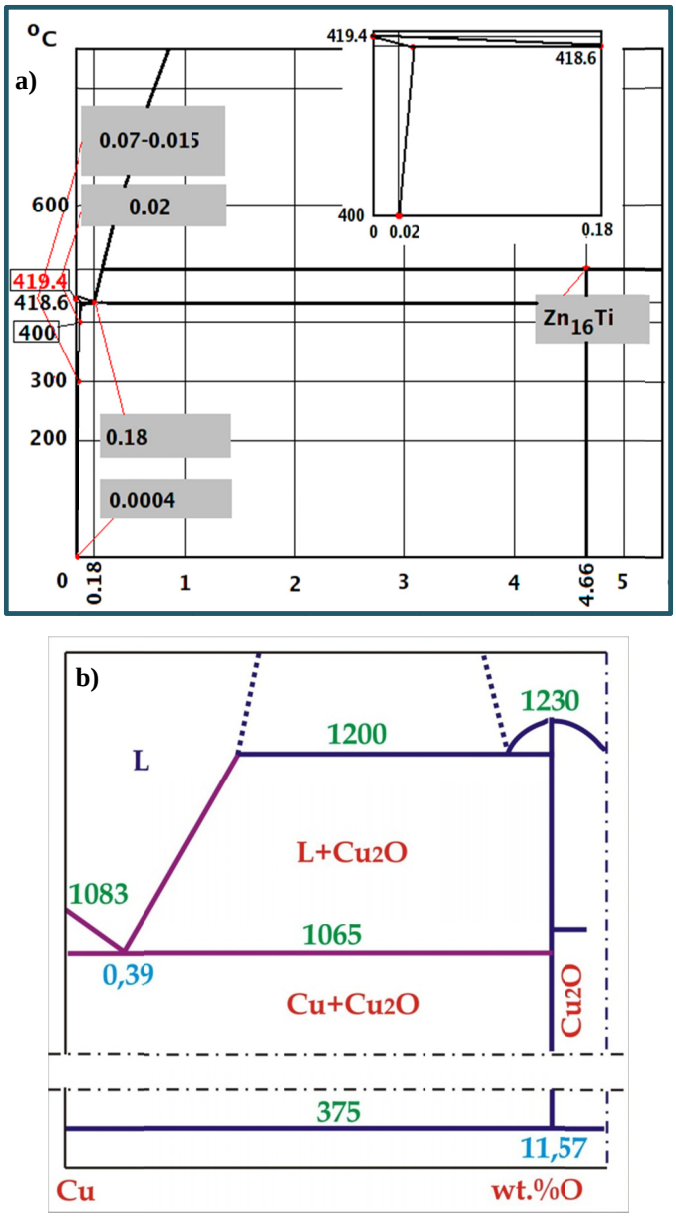

Fig. 4. Phase diagram for stable equilibrium, a) Zn-Ti, [11]; b) Cu-O, [12], [°C/wt.%]

The $Zn_{16}Ti$ – intermetallic compound is the *faceted* phase. Its crystallographic parameters are: a = 7.720; b = 11.449; c = 11.775 [A], [13]

The performed experiments show that the $Zn_{16}Ti$ – intermetallic compound can be easily exposed in the strengthening layers, Fig. 5-6.

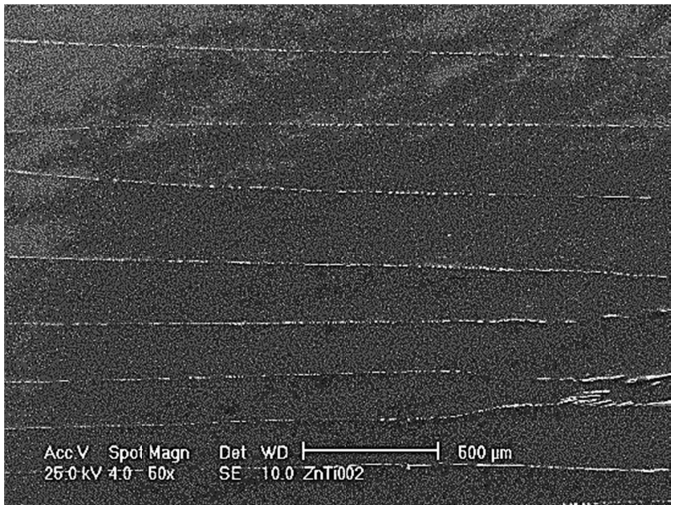

Fig. 5. Strengthening layers which contain the $Zn_{16}Ti$ – intermetallic compound

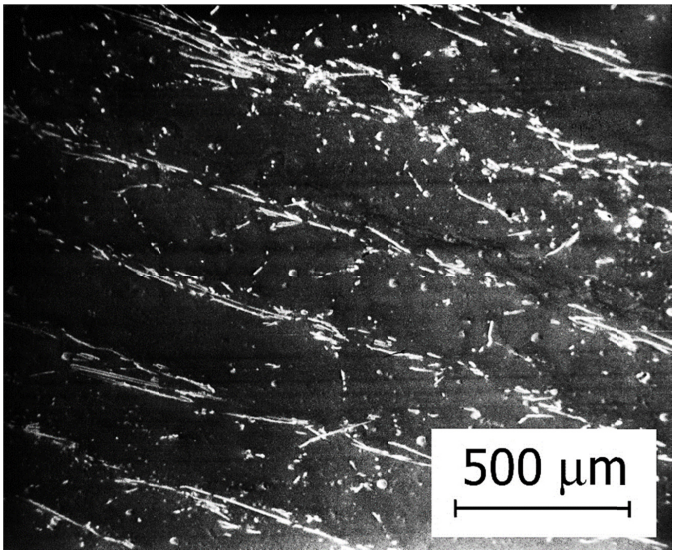

Fig. 6. The $Zn_{16}Ti$ – intermetallic compound (bright) in strengthening layers created within the (Zn) – single crystal

In the case of the so-called equilibrium solidification (Lever Rule), there is no possibility to form strengthening layers of eutectic composition in the first -, and second alloy, Fig. 1-2, respectively. The strengthening layers are formed when the nominal alloy concentration is equal to that shown in Fig. 3. The precipitate which appears in this situation is the $i_E(N_0)|_{\alpha=1}$ – equilibrium eutectic only, [14]. However, the equilibrium solidification is not a feasible process, therefore the non-equilibrium solidification occurs in the industry / laboratory conditions, only. Then, eutectic precipitate is expected even in the first alloy of the "I" – solute, Fig. 1. This would be the $i_D(\alpha, N_0)$ – non-equilibrium precipitate.

The interlayer distance is constant, Fig. 6, for the imposed growth rate and nominal solute concentration. Nevertheless, the width of the layer can be modified through changing of the growth rate and the resultant appearance of the adequate amount of the non-equilibrium eutectic precipitate. The higher is crystal growth rate, the more significant is deviation from the equilibrium solidification and the bigger is amount of the non-equilibrium precipitate. Some changes of growth rate influence the diffusion which is a time-consuming phenomenon. Therefore, diffusion has limited possibilities to form a diversified / subtle layer morphology when the growth rate is elevated significantly. Thus, some structural transformations are expected within the layers with the increasing growth rate, [3,15,16]. Eventually, an interlayer spacing, a layer width, and the actual morphology of a given layer are to be considered, Fig. 7.

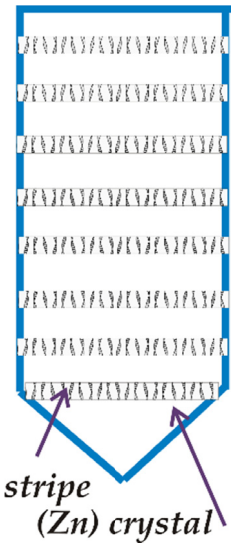

Fig. 7. Schematic outline of a single crystal decorated with stripes (strengthening layers) of constant spacing and width, and the morphology relevant to an imposed growth rate

Some changes in the mentioned parameters were observed in function of the v – growth rate for three imposed nominal Ti – solute concentrations. The applied growth rates were situated within the range: $0 < v \leq 16$ [mm/h]. The thermal gradient created at the s/l interface of the growing single crystal was equal to: $G \approx 80$ [K/cm]. The ingots of the ZnTi0.01, ZnTi0.02 and ZnTi0.1 [wt.%] alloys, with and without copper addition, were prepared as a charge to the *Bridgman's* system. The size of the produced (Zn) – single crystals was: 26×6×120 [mm].

When a given nominal solute concentration is fixed, controlling the layers width is possible only by the selection of the growth rate, v. It is obvious as the imposed growth rate, v, determines the value of the $\alpha(v)$ – back-diffusion parameter during solidification, [5], and consequentially the amount of non-equilibrium precipitate. The layers appear periodically in the (Zn) – single crystal in a cyclical manner with the F – interlayer distance which is constant during solidification, Fig. 8.

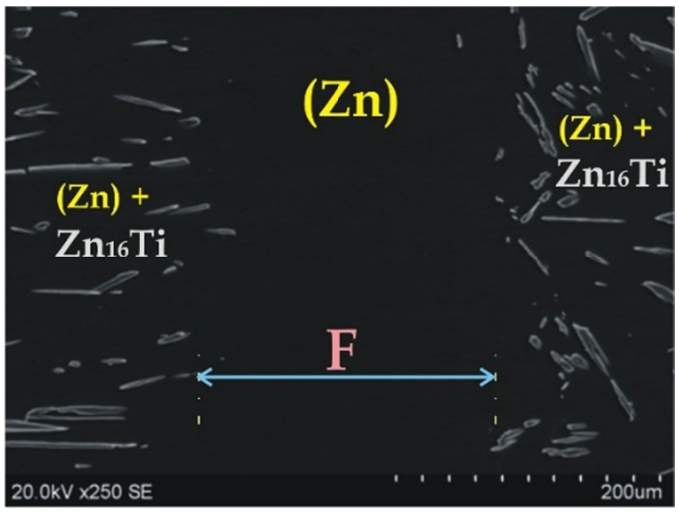

Fig. 8. Inter-layer distance, F, created periodically within the (Zn) – crystal strengthened by the E = (Zn) + $Zn_{16}Ti$ – eutectic precipitate (in fact, by the $Zn_{16}Ti$ – intermetallic compound)

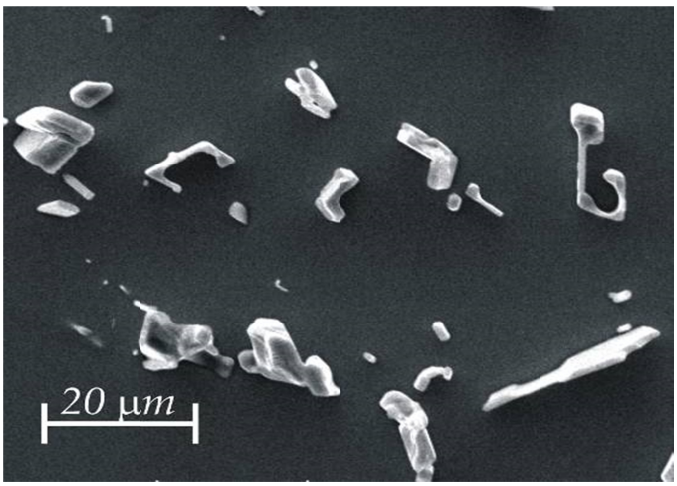

Fig. 9. L-shape rod-like structure formed in the strengthening layers within the $0 \leftrightarrow v_1$ – range of growth rates applied to the *Bridgman's* system; the irregular eutectic in which the $Zn_{16}Ti$ – compound forms some branches

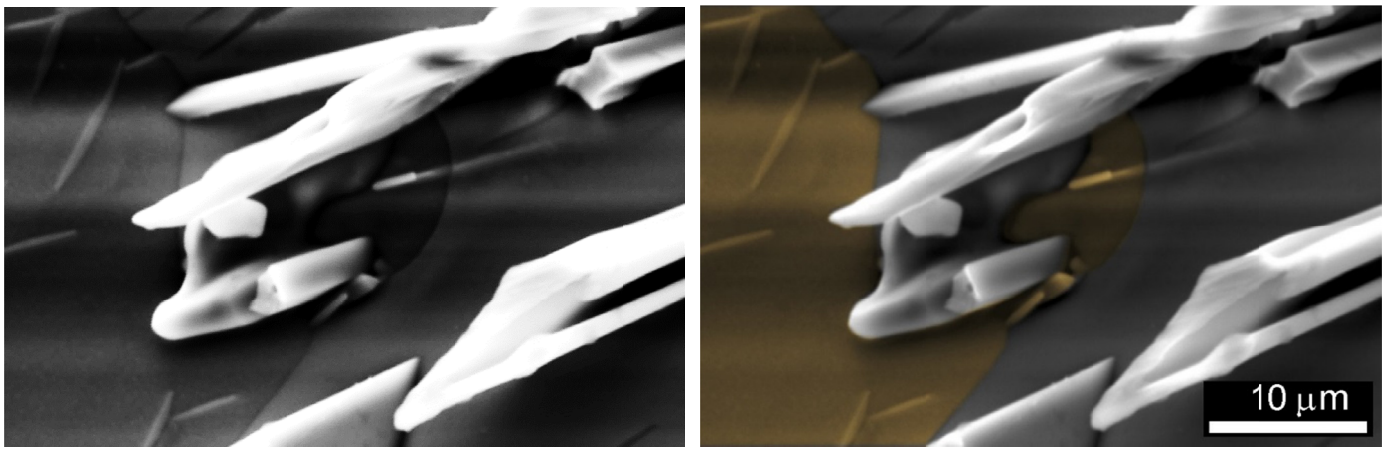

Fig. 10. Phenomenon of branching recorded in the irregular L-shape, rod-like eutectic structure; almost plane s/l interface exposed between main rod and its branch: a) structure without any correction, b) new color superposed over the frozen liquid to make the planar s/l interface well-marked

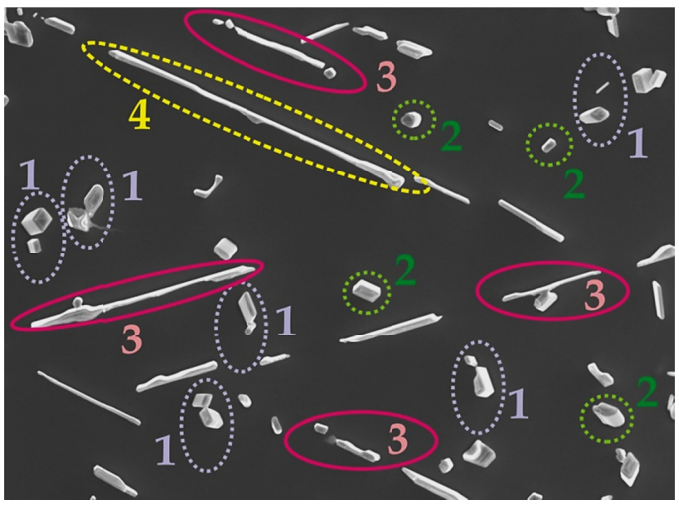

Fig. 11. Co-existence of different forms of the $Zn_{16}Ti$ – compound as observed within the $v_1 \leftrightarrow v_1'$ – range of growth rates: 1) – transformation of irregular branched rods into regular rods (vanishing of branches); 2) – regular rods as a result of the "1" – structural transformation; 3) – transformation of regular rod into regular lamella; 4) – fully shaped regular lamella after the completed transformations

Two morphological transitions were recorded owing to performed experiments. At the v_1 – threshold growth rate, the L-shape rod-like structure, Fig. 9, begins to take shape of a regular lamellar one. However, the mentioned rod-like morphology is an irregular eutectic structure equipped with some branches, Fig. 10, which vanish within a certain range of growth rates, $v_1 \leftrightarrow v_1'$. This is not a sharp transformation but rather a slow-going continuous modification, Fig. 11. Regular rods appear first as branches vanish. Then, the regular rods transform into regular lamellae. Consequentially, the regular lamellae can co-exist together with irregular and regular rods when a given growth rate (or local growth rate) fulfils the following condition, $v_1 < v < v_1'$, Fig. 11.

Next, regular lamellae which are observed within the $v_1' \leftrightarrow v_2$ range of growth rates, Fig. 12, transform into regular rods at the v_2 – threshold growth rate, Fig. 13. This is strictly a sharp transformation.

A regular rod-like structure appears within the strengthening layers when the growth rates range is as follows: $v_2 \leftrightarrow v_3$, Fig. 14.

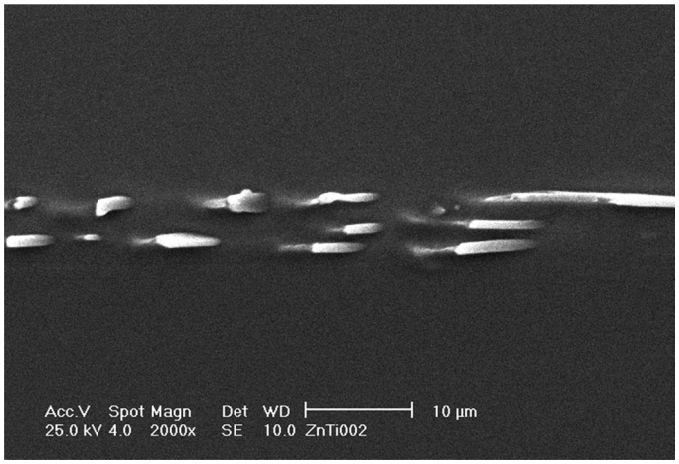

Fig. 12a. Regular lamellae observed within the $v_1' \leftrightarrow v_2$ – range of growth rates

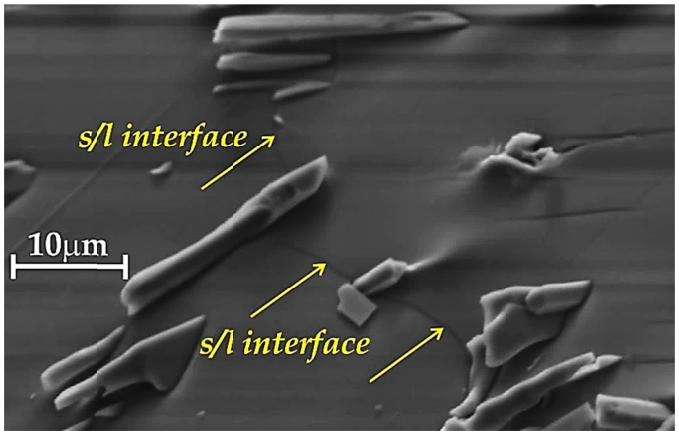

Fig. 12b. Parabolic shape of the *s*/*l* interface typical for regular, lamellar structure

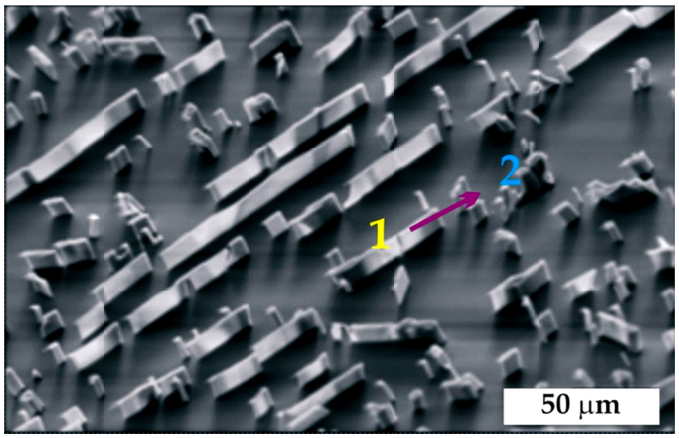

Fig. 13. Disintegration of lamellae into rods (("1") ⇒ ("2")) during the transformation at the v_2 – threshold growth rate; "1" – lamella just before disintegration; "2" – disintegrated lamella

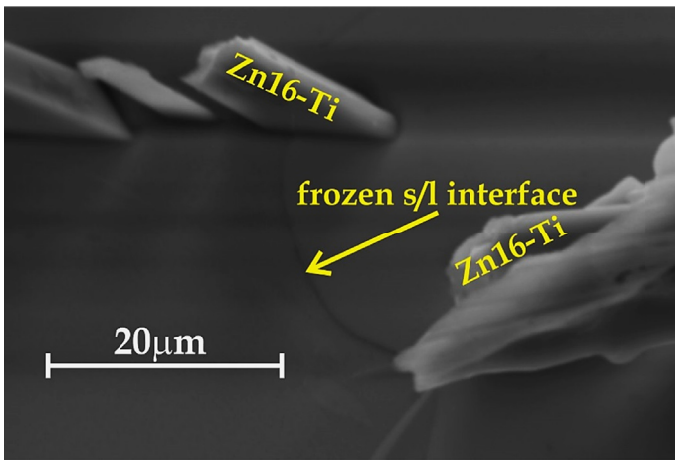

Fig. 14a. Parabolic shape of the s/l interface of the (Zn) – *non-faceted* phase for regular rod-like structure formation

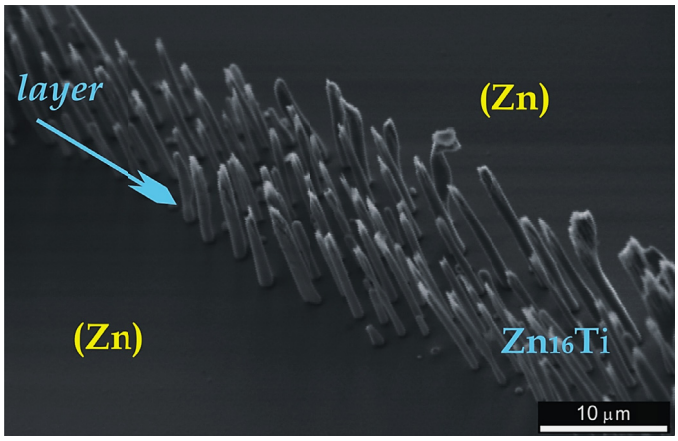

Fig. 14b. Protrusion of the rods of the $Zn_{16}Ti$ – intermetallic compound (leading phase) above the (Zn) – phase (wetting phase) within the strengthening layer

The formation of the strengthening layers which contain either regular or irregular eutectic structure is limited. When the imposed growth rate is beyond the v_3 – threshold rate, then the (Zn) – single crystal evinces a "honey-comb" morphology with the rod-like structure in precipitates. When the growth rate is close to the v_3 – growth rate, ($v > v_3$), formation of the strengthening structural lines is accompanied by appearing of the structural "bridges" which connect these structural "lines", Fig. 15. The structural "bridges" become as wide as structural "lines" with the increasing growth rate, ($v \gg v_3$), Fig. 16.

The $Zn_{16}Ti$ – intermetallic compound protrusion above the (Zn) – matrix is visible not only in the strengthening layers, Fig. 13, Fig. 14, but in the strengthening "lines" and "bridges" as well, Fig. 17. The protrusion is associated with the growth rate, v. The higher is growth rate, v, the smaller is protrusion, d, as proved theoretically, [17].

The threshold growth rates (in agreement with the performed experiments) are as follows: $v_1 \approx 5$; $v_1' \approx 5.8$; $v_2 \approx 10$; $v_3 \approx 16$ [mm/h].

3. Thermodynamics of the stationary pattern formation

Thermodynamics of eutectic morphologies formation has already been analyzed in correlation with the entropy of solu-

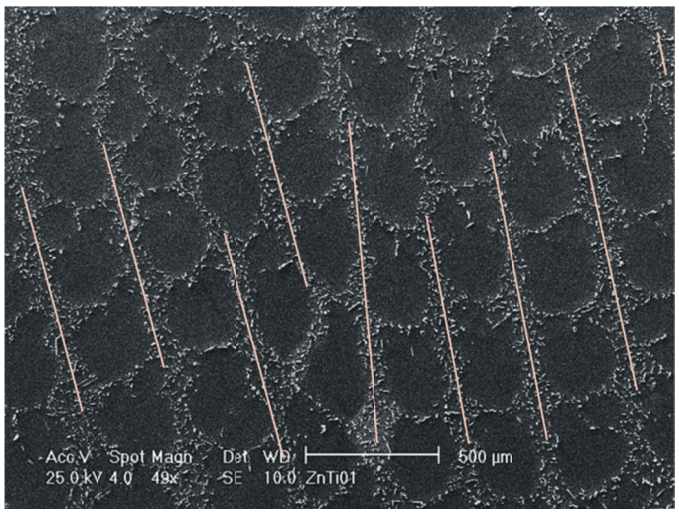

Fig. 15a. Strengthening "lines" connected by means of the so-called structural "bridges" (colored lines superposed over the structural lines)

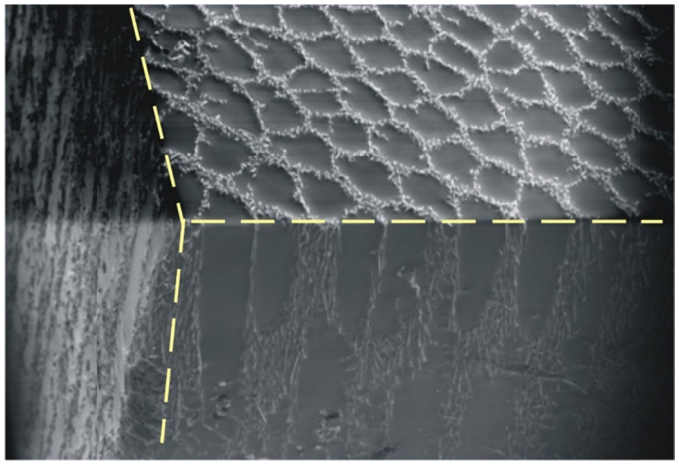

Fig. 15b. 3D – visualization of the (Zn) – single crystal morphology

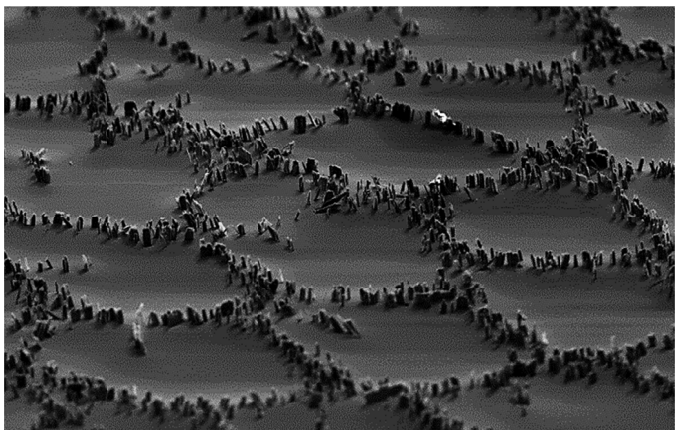

Fig. 16. Fully shaped "honey-comb" morphology of the (Zn) – single crystal; structural "bridges" width is equal to the width of structural "lines"

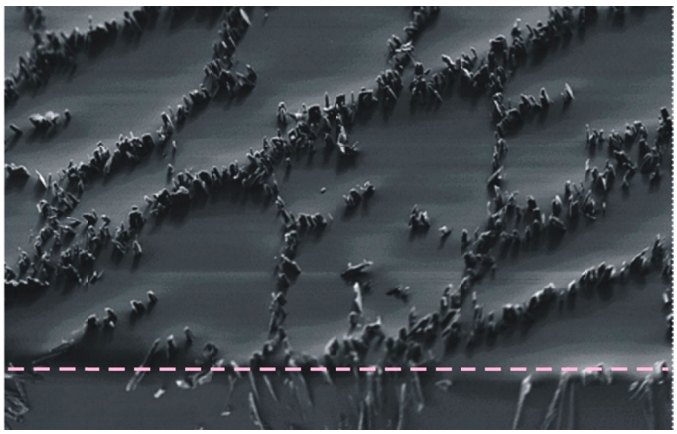

Fig. 17. Cross -, and longitudinal section of the (Zn) – single crystal presenting the "honey-comb" morphology; visible both rod-like structure on the longitudinal section and the $Zn_{16}Ti$ – compound protrusion on the cross-section

tion for the intermetallic compound which constitutes one of the eutectic phases, [18]. This theory is not able to explain the eutectic morphologies competition. It makes however a good contribution to the eutectic classification.

By the means of experiment, one and only one spacing is obtainable in a given eutectic structure formed under stationary state when a given growth rate, v, is imposed on the system, [19]. Therefore, a certain criterion to control stationary state and resulting structural parameters must be applied to the mathematical / thermodynamic description of solidification. This way, this criterion optimizes the course of solidification process. It is assumed that the $dP \leq 0$ – *general evolution criterion*, [20], is to be considered in the current description to determine stationary state for solidification under investigation.

First of all, however, the theorem of *minimum entropy production* should be mentioned. The P – entropy production per unit time is expressed as a function of the σ – entropy production per unit time and unit volume, [20,21].

$$P = \frac{d_i S}{dt} = \int_V \sigma \, dV \geq 0 \tag{1}$$

with

$$d_i S = dS - d_e S \tag{1a}$$

In the above relationship, the difference between the dS – total entropy change and the $d_e S$ – entropy "exchange" with the outside environment yields the $d_i S$ – second part of the total entropy change which is connected with irreversible processes generated in the envisaged system (in the V – volume, that is in the macroscopic point in which all fundamental forces and fluxes can be considered / observed). On the other hand, the σ – entropy production per unit time and unit volume is a bilinear form for the X_i – generalized forces, and the J_i – generalized fluxes (rates) of the irreversible processes:

$$\sigma = \sum_i J_i \, X_i \geq 0 \tag{2}$$

It can be proved that under certain restrictive conditions (also with validity of the *Onsager's* reciprocity relations) the entropy production can only decrease for time independent boundary conditions: $dP \leq 0$, [20]. Thus, $P \Rightarrow$ minimum, at

the stationary state itself. This condition (*minimum entropy production*) is applied to the current description of the eutectic morphologies formation /competition as the criterion which optimizes the structural spacing and additionally the winning pattern appearance.

The $dP \leq 0$ – *general evolution criterion* can be extended. At first, it is necessary to split the entropy production, Eq. (2) into two parts, [20,22]:

$$d\sigma = d_X\sigma + d_J\sigma \tag{3}$$

where, the $d_X\sigma$ – differential, Eq. (3), is the contribution to entropy production due to the generalized thermodynamic forces, whereas, $d_J\sigma$, is the contribution to entropy production due to the generalized thermodynamic fluxes:

$$d_X\sigma \equiv \sum_i J_i\, dX_i \text{ and } d_J\sigma \equiv \sum_i X_i\, dJ_i \tag{4}$$

By analogy to Eq. (3):

$$dP = d_X P + d_J P \tag{5}$$

where, the $d_X P$ – differential, Eq. (5), is the contribution to the P – entropy production due to the generalized thermodynamic forces, whereas, $d_J P$, is the contribution to the P – entropy production due to the generalized thermodynamic fluxes considered for the system as a whole.

It was shown, that for time independent boundary conditions the inequality:

$$d_X P = \int dV \sum_i J_i\, dX_i \leq 0 \tag{6}$$

is always satisfied during evolution of a given system without any references to the phenomenological relations binding the J_i – generalized rates to the X_i – generalized forces. The inequality, Eq. (6), is known as the so-called *universal evolution criterion*, [23].

The *universal evolution criterion* remains valid for nonlinear processes while the $P \Rightarrow$ minimum theorem is a particular case of linear processes for which:

$$d_X P = d_J P = 0.5 dP \tag{7}$$

In the phenomenological formulation:

$$\delta_X P = \sum_{ik} L_{ik}\, X_k\, \delta X_i \tag{8}$$

It was proved, with the use of the *Onsager's* reciprocity relations, [24], that:

$$\delta_J P = \sum_k X_k\, \delta J_k = \sum_{ik} X_k \left(L_{ik}\, \delta X_i\right) = \delta_X P \tag{9}$$

which justifies validity of Eq. (7).

3.1. Entropy production per unit time and unit volume

The (Zn) – single crystal growth proceeds in a stationary state in the *Bridgman's* system with constant both the v – growth rate and $G = \partial T/\partial z$ – thermal gradient. Thus, the application of the theorem of *minimum entropy production* is assumed in this situation. The σ – entropy production per unit time and unit volume should be considered with regard to the mass transfer in the liquid and heat transfer in the solid in some proper zones touching the s/l interface ($\sigma = \sigma_D + \sigma_T$). However, heat transfer is the phenomenon much more rapid in comparison with diffusion, [22]. Therefore, heat transfer has negligible contribution to entropy production. Finally, it is reasonable to consider the effect of the diffusion on the entropy production in such a system.

The current model considers only a binary eutectic alloy. Thus,

$$J_1 = -J_2 = J_C, \text{ and } X_1 = -X_2 = X_C \tag{10}$$

The J_C – flux of diffusion is strictly associated with the X_C – thermodynamic force. In the considered case, the X_1, X_2 – thermodynamic force is defined through the $\bar{\mu}_i$ – chemical potential of the i-th element of an alloy:

$$X_i = -grad.\frac{\bar{\mu}_i}{T}, \quad i = 1,2 \tag{11}$$

The entropy production per unit time and unit volume is given now as:

$$\sigma_D = \frac{1}{T}\left[J_1(-grad.\bar{\mu}_1) + J_2(-grad.\bar{\mu}_2)\right], \quad \sigma_T = 0 \tag{12}$$

The applicability of the *Fick's* law in the considered system is justified.

$$J_i = -D\, grad.N_i \tag{13}$$

Consequentially,

$$\sigma_D = -\frac{D}{T} grad.N_1\left[(-grad.\bar{\mu}_1) - (-grad.\bar{\mu}_2)\right] \tag{14}$$

The $\bar{\mu}_i$, (i = 1,2) – chemical potential is defined:

$$\bar{\mu}_i = \mu_0^i + R_g\, T \ln\left(\gamma_i\, N_i\right) \tag{15}$$

with, γ_i – activity coefficient of the i-th element in a given solution, R_g – gas constant, and μ_0^i – standard chemical potential, T – is assumed to be temperature of the isothermal *s/l* interface.

The above assumption ($T = T_{s/l} = const.$) results in the following definition of the chemical potential gradient:

$$grad.\bar{\mu}_i = R_g\, T\left(\frac{\partial \ln \gamma_i}{\partial N_i}\frac{dN_i}{dz} + \frac{\partial \ln N_i}{\partial N_i}\frac{dN_i}{dz}\right) \tag{16}$$

$$grad.\bar{\mu}_i = R_g\, T\left(\frac{\partial \ln \gamma_i}{\partial \ln N_i}\frac{1}{N_i}\frac{dN_i}{dz} + \frac{1}{N_i}\frac{dN_i}{dz}\right) \tag{17}$$

$$grad.\bar{\mu}_i = R_g\, T\left\{\frac{1}{N_i}\left[1+\frac{\partial \ln \gamma_i}{\partial \ln N_i}\right]\frac{d\,N_i}{d\,z}\right\},\ i=1,2 \qquad (18)$$

$\frac{\partial \ln \gamma_i}{\partial \ln N_i}$, can be determined from one of the possible solutions to the *Gibbs-Duhem's* rule. According to the *Gibbs-Duhem's* rule:

$$N_1 d\ln\gamma_1 + N_2 d\ln\gamma_2 = 0 \qquad (19)$$

The following solution to the *Gibbs-Duhem's* rule, [25], is suggested:

$$\ln\gamma_i = f(T)\,f(N_i),\ N_1+N_2=1 \qquad (20)$$

$$f(T) = \bar{\alpha}\,T^{-1} + \bar{\beta} + \bar{\eta}\,T^{-2} \qquad (21)$$

The $\bar{\alpha}; \bar{\beta}; \bar{\eta}$ – coefficients serve to approximate / optimize Eq. (21), and:

$$f(N_1) = (1-N_1)^{m'} \qquad (22a)$$

$$f(N_2) = {N_2}^{m'} - \frac{m'}{m'-1}{N_2}^{m'-1} + \frac{1}{m'-1} \qquad (22b)$$

or,

$$f(N_1) = {N_1}^{m'} - \frac{m'}{m'-1}{N_1}^{m'-1} + \frac{1}{m'-1} \qquad (23a)$$

$$f(N_2) = (1-N_2)^{m'} \qquad (23b)$$

The m' – parameter is selected empirically (Eq. (22), Eq. (23)), and generally should satisfy the following inequality: $1 < m' < 2$, [25]. Subsequently,

$$\frac{\partial \ln \gamma_i}{\partial \ln N_i} = f(T)\frac{d\,f(N_i)}{d\ln N_i} = f(T)\frac{d\,f(N_i)}{dN_i}N_i \qquad (24)$$

Eq. (18) can be rewritten:

$$grad.\bar{\mu}_i = R_g\, T\frac{1}{N_i}\varepsilon\, grad.N_i,\ \ 1+\frac{\partial \ln \gamma_i}{\partial \ln N_i} = \varepsilon \qquad (25)$$

Combination of Eq. (25) with Eq. (14) yields:

$$\sigma_D = -DR_g\,\varepsilon\, grad.N_1\left[\frac{-grad.N_1}{N_1} - \frac{-grad.N_2}{N_2}\right] \qquad (26)$$

$$\sigma_D = -DR_g\,\varepsilon\, grad.N_1\left[\frac{-(1-N_1)\,grad.N_1 + N_1 grad.(1-N_1)}{N_1(1-N_1)}\right] \qquad (27)$$

Finally, after some rearrangements and in a general form, [22], entropy production associated with the mass transfer only, ($\sigma_T = 0$), is given as follows:

$$\sigma_D = \frac{DR_g\,\varepsilon}{N_i(1-N_i)}\left|grad.N_i\right|^2 \quad T \equiv T_{s/l} = const. \qquad (28)$$

Eq. (28) presents the definition of the entropy production per unit time and unit volume. Eq. (28) is ready to be introduced into Eq. (1) in order to calculate entropy production per unit time, separately for lamellar -, and rod-like eutectic structure formation within the layers strengthening the (Zn) – single crystal.

3.2. Entropy production per unit time

The current description is connected with the mass transfer in the liquid adjacent to the *s/l* interface but contained in the diffusion zone: $z_D \approx D/v$ (in the z – direction), [26]. Entropy production associated with the heat transfer is neglected, Eq. (28). Therefore, Eq. (1) is to be rewritten:

$$P_D = \int_V \sigma_D\, dV \qquad (29)$$

The V – volume is the key parameter for the subsequent calculation / solution of the integral, Eq. (29). It leads to the separation of integration which now, will be made simultaneously for the lamellar -, and rod-like structure formation. The V – volume is defined in Fig. 18a for the lamellar -, and in Fig. 18b for the rod-like structure formation.

The V – volume is reproduced periodically in the regular eutectic morphology. However, this volume is not the same for every new solidification rate. Therefore, the average entropy production could be calculated:

a) for the lamellar eutectic growth

$$\bar{P}_D^L = \frac{1}{S_\alpha + S_\beta}\int_V \sigma_D\, dV \qquad (30a)$$

b) for the rod-like eutectic growth

$$\bar{P}_D^R = \frac{1}{\pi(r_\alpha + r_\beta)^2}\int_V \sigma_D\, dV \qquad (30b)$$

Eq. (31) is obtained by introducing Eq. (28) into Eq. (29):

$$P_D = \frac{DR_g\,\varepsilon}{N_i(1-N_i)}\int_V \left|grad.N_i\right|^2 dV \qquad (31)$$

4. Concluding remarks

The current theory proves that morphological transformations observed within the layers strengthening the (Zn) – single crystal have the thermodynamic background. Since the experiment was performed under stationary state, the only criterion which could be used in such a model is the theorem of *minimum entropy production*. Therefore, entropy production per unit time and unit volume is delivered. Subsequently, the entropy production per unit time should be calculated for the both morphologies formation and subsequently, subjected to the minimization. Then, the application of the postulated criterion:

in the structural – thermodynamic competition the winner is this kind of the pattern for which minimum entropy production is lower,

is proposed to be verified in the next parts of the current model.

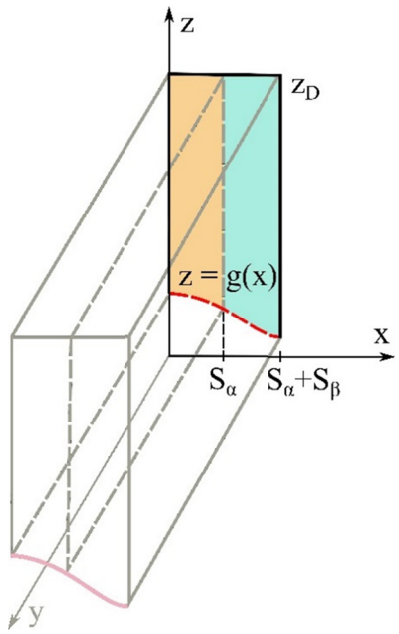

Fig. 18a. The V – volume applied to Eq. (29) for the lamellar structure formation; the $z = g(x)$ – function describes the s/l interface curvature (red dashed line)

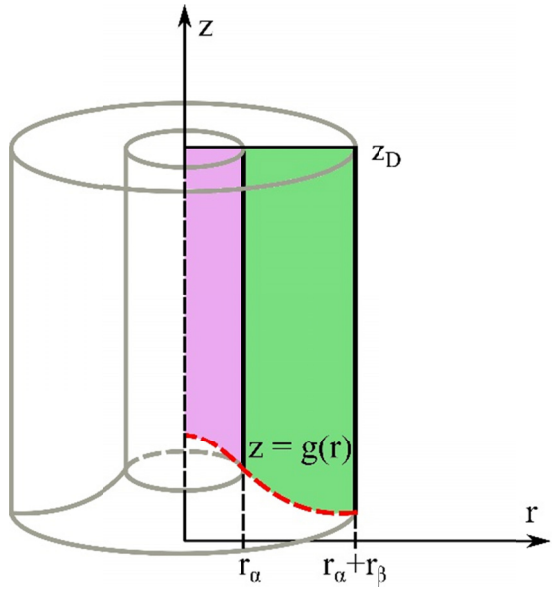

Fig. 18b. The V – volume applied to Eq. (29), for the rod-like structure formation; the $z = g(r)$ – function describes the s/l interface curvature (red dashed line)

This verification can be obtained by:

a) analysis of the Zn-$Zn_{16}Ti$ phase diagram and some accompanying experiments performed within four ranges of the growth rates,
b) detailed calculation of the entropy production per unit time for both examined eutectic structures,
c) development of the *Growth Law* for both eutectic structures appearance,
d) application of the concept of marginal stability to define the *operating range* for the irregular eutectic structure formation,
e) descriptions of both irregular – into regular structure transformation (debranching), and regular rod-like -, into regular lamellar structure transformation,
f) examination of the newly developed theory for the solute micro-field formation with the verification of the local mass balance which allows to display the leading phase protrusion.

The entropy production per unit time and unit volume, Eq. (28), has been determined for the isothermal *s*/*l* interface. The geometry of this isothermal interface should be bound with the shape of the transition layer, [27].

Calculation of the entropy production per unit time, Eq. (29), is currently limited to the entropy production associated with the mass transfer only. It is self-explanatory because heat transfer runs very quickly in comparison with the mass transfer. Thus, contribution of the heat transfer to the entropy production is negligible, [19].

Moreover, calculation of the entropy production per unit time, Eq. (29), is performed for the $0 \le z \le z_D$ – boundary layer, where, $z_D \approx D/v$.

Acknowledgements

The support was provided by the National Center for Research and Development under Grant No. PBS3/A5/45/2015.
The assistance of Professor G. Boczkal – AGH University of Science and Technology, Kraków, is greatly appreciated.

REFERENCES

[1] G. Boczkal, Materials Science Forum **674**, 245-249 (2011).
[2] W. Wołczyński, B. Mikułowski, G. Boczkal, Materials Science Forum **649**, 125-130 (2010).
[3] W. Wołczyński, International Journal of Thermodynamics **13**, 35-42 (2010).
[4] W. Wołczyński, Archives of Metallurgy and Materials **58**, 309-313 (2013).
[5] N.F. Mott, F.R.N. Nabarro, Proceedings of the Physical Society **52**, 86-89 (1940).
[6] A. Kelly, M.E. Fine, Acta Metallurgica **5**, 365-367 (1957).
[7] D. Dew-Huges, W.D. Robertson, Acta Metallurgica **8**, 147-155 (1960).
[8] J.G. Byrne, M.E. Fine, A. Kelly, Philosophical Magazine **6**, 1119-1145 (1961).
[9] R. Ebeling, M.F. Ashby, Philosophical Magazine **13**, 805-834 (1966).
[10] N. Zarubova, B. Sestak, Physica Status Solidi **30**, 365-374 (1975).
[11] J.L. Murray, Phase Diagram of Binary Titanium Alloys, Ed. ASM International, Metals Park, Ohio, 336-339 (1987).
[12] L. Schramm, G. Behr, W. Loser, K. Wetzig, Journal of Phase Equilibria and Diffusion **26**, 605-612 (2005).
[13] G. Boczkal, Archives of Metallurgy and Materials **58**, 1019-1022 (2013).

[14] W. Wołczyński, Back-Diffusion Phenomenon during the Crystal Growth by the Bridgman Method, chapter 2 in the book: Modelling of Transport Phenomena in Crystal Growth, Ed. J.S. Szmyd & K. Suzuki; WIT Press: Southampton/UK – Boston/USA, 19-59 (2000).
[15] S. Khan, A. Ourdjini, R. Elliott, Materials Science and Technology **8**, 516-524 (1992).
[16] B. Toloui, A. Hellawell, Acta Metallurgica **24**, 565-573 (1976).
[17] W. Wołczyński, Defect and Diffusion Forum **272**, 123-138 (2007).
[18] R.S. Fidler, M.N. Crocker, R.W. Smith, Journal of Crystal Growth **13/14**, 739-746 (1972).
[19] G. Lesoult, Journal of Crystal Growth **13/14**, 733-738 (1972).
[20] P. Glansdorff, I. Prigogine, Physica **30**, 351-374 (1964).
[21] S. Kjelstrup, D. Bedeaux, Non-Equilibrium Thermodynamics of Heterogeneous Systems. World Scientific Publishing Co. Ltd., Ed. M. Rasetti, New Jersey/USA – London/UK – Singapore – Beijing; Shanghai/China – Hong-Kong – Taipei/Taiwan – Chennai/India, (2008).
[22] G. Lesoult, M. Turpin, Memoires Scientifiques de la Revue de Metallurgie **66**, 619-631 (1969).
[23] P. Glansdorff, I. Prigogine, Physica **46**, 344-366 (1970).
[24] I. Prigogine, Introduction a la Thermodynamique des Processus Irreversibles, Monographies DUNOD, Paris/France, (1968).
[25] A. Krupkowski, Fundamental Problems of the Theory for Metallurgical Processes, PWN, Warszawa/Poland, (1974).
[26] W. Kurz, D.J. Fisher, Fundamentals of Solidification, Trans Tech Publications Ltd, Uetikon-Zuerich/Switzerland, (1998).
[27] W. Wołczyński, Crystal Research and Technology **25**, 1433-1437 (1990).